World Journal of Advanced Research and Reviews
eISSN: 2581-9615 CODEN (USA): WJARAI
Cross Ref DOI: 10.30574/wjarr
Journal homepage: https://wjarr.com/

(RESEARCH ARTICLE)

Check for updates

Numerical modeling of the magneto convection of a Newtonian fluid confined between two vertically eccentric hemispheres

Fallou Sarr *, Vieux Boukhaly Traore, Omar Ngor Thiam and Mamadou Lamine Sow

Department of Physics, Faculty of Science and Technology, Cheikh Anta DIOP University, Dakar, Senegal.

World Journal of Advanced Research and Reviews, 2022, 16(02), 893–907

Publication history: Received on 10 October 2022; revised on 19 November 2022; accepted on 22 November 2022

Article DOI: https://doi.org/10.30574/wjarr.2022.16.2.1229

Abstract

This work is a contribution to the numerical study of the phenomenon of heat transfer by laminar natural convection of an electrically conductive Newtonian fluid subjected to a uniform horizontal magnetic field. The study focused on a hemispherical cavity delimited by two vertically eccentric hemispheres. A constant flux density is imposed on the inner hemisphere while the outer hemisphere is maintained at a constant temperature. The combination of thermal and electrical boundary conditions is exploited to obtain the critical values of the parameters marking the onset of instability. The Boussinesq approximation is used to study the equations governing this fluid instability. The projection of these equations in the bispheric coordinate system as well as the discretization by the finite difference method facilitated the development of a computer code in Fortran. The exploitation of this code made it possible to determine the growth rates for Hartmann values equal to 1; 10 and 100, from Rayleigh equal to 10^3; 10^4; 10^5 and 10^6, with eccentricity equal to ± 0.2; ± 0.5 and 0 and a radius ratio equal to 2. The aim is to highlight the effect of the magnetic field on the heat transfer. At the end of the study, the results obtained are consistent and revealing: they are in good agreement with those of references drawn from the literature.

Keywords: Magneto convection; Magnetic field; Hemispherical cavity; Eccentricity; Rayleigh Correlations; Hartman Number; Nusselt Number

1. Introduction

The effect of the magnetic field in liquid metals, commonly called magneto-convection, has been the subject of a large number of researches in recent decades [1]. The interest of these materials lies in their involvement in several natural and applied phenomena [2]. According to [3], magneto-convection has several applications in various fields such as: geophysics, astrophysics, plasma physics, missile technology, medicine, biology etc. Thus, at various configurations and in parallel with studies on pure natural convection, numerous experimental and numerical studies on the magneto-convection of a fluid confined in enclosures have been made [4]. The latter generally have very varied geometries and sometimes parallelepipedal [5, 6], cylindrical [7, 8], or even spherical [9, 10, 11, 12]. In this sense, correlations giving Nusselt and Rayleigh numbers are sometimes proposed; an increase in such numbers, that is to say intensification of natural convection, or of the magnetic field, must be able to influence, depending on the geometry of the walls, the viscosity of the fluid and the stability of the flows [13, 14]. Thus, by modeling for a magneto-convection, the effects of the discretization method, the refinement and the stretching of the grid, the results of [6] prove that in addition to stabilizing the main convection roll, the field Horizontal magnetic makes it also comes with higher kinetic energy and heat transfer rate if we compare the study with a non-magnetic case. The analysis of Hall effects of magneto-convective instability and heat transfer exploited by [15], studies parameters that can influence the flow field and the temperature distribution. According to their results, Hall currents significantly decrease the flow field. [16] and [17] attempted to acquire a general and essential understanding of the flows and heat transfer characteristics in an enclosure in the

* Corresponding author: Fallou Sarr
Department of Physics, Faculty of Science and Technology, Cheikh Anta DIOP University, Dakar, Senegal.

presence of a magnetic field. Their studies showed that the magnetic field decreases the rate of heat transfer. The effect of the magnetic field in mixed convection, with an exponential temperature distribution in the presence of a magnetic field and with thermal and internal viscous dissipation has been studied by [18]. It was found that increasing the Prandtl number decreases the coefficient of skin friction, while increasing the magnetic field increases the local Nusselt number. The study of the transient regime of the natural convection of a non-conductive Newtonian fluid located between two vertically eccentric spheres, the internal sphere of which is subjected to a heat flow of constant density, the external sphere being isothermal have been developed in the literature. by [9]. Their results show that the increase in the modified Rayleigh number makes it possible to reach the steady state more quickly and that the influence of eccentricity is very weak on the establishment of the equilibrium state. The convection movement is reinforced for positive eccentricities. The heat exchange characterized by the Nusselt number increases with the modified Rayleigh number. [19] studied the case of a hemisphere. The results show that the center of the vortex moves upwards for larger eccentricities. The Nusselt number increases with the modified Rayleigh number. When the latter increases, the dimensionless temperature decreases for a given eccentricity. This wealth of literature testifies to the importance and the scientific scope relating to the thermal convection of an electrically conductive fluid subjected to a magnetic field [20]. Moreover, it is in this same order of idea that the present study was initiated. Our study concerns the natural convection between two eccentric hemispheres of a conductive fluid subjected to a magnetic field. It is a question of studying in transient regime the magneto-convection of a Newtonian fluid subjected to a horizontal magnetic field confined between two vertically eccentric hemispheres. For this purpose, a constant flux density is imposed on the inner hemisphere while the outer hemisphere is maintained at a constant temperature. The main object is on the one hand, to determine the influence of the magnetic field on the isotherms and the lines of current and on the other hand the influence of the number of Hartmann on the number of Nusselt, the function of current and on temperature.

2. Material and methods

2.1. Problem formulation

Figure 1 symbolizes a movement of an electrically conductive Newtonian fluid (humid air) subjected to a horizontal magnetic field and confined in an annular space delimited by two vertically eccentric hemispheres. The radii of the internal and external hemispheres are denoted respectively by Ri and Re. The algebraic value of the distance separating the centers of these two hemispheres is defined as being the eccentricity e'. Inside and on the walls of the enclosure, the temperature is initially uniform. A heat flux (q') of constant density will be applied at the level of the internal hemisphere while the temperature of the external hemisphere will remain constant (T'). The walls which separate the two hemispheres at the angles θ=0 and θ= π are adiabatic. A transient natural convection of this conductive fluid caused by the temperature difference of the two hemispheres will develop inside the domain. The physical properties of the fluid are constant except its density in the term associated with gravity in the equation of motion where it varies linearly with temperature and obeys Boussinesq's law. The fluid is Newtonian and the flow is laminar, incompressible and two-dimensional. The magnetic field is assumed to be constant and the induced field is neglected. The viscous dissipation function, the radiative effects as well as the pressure term are neglected. The boundaries of the studied system are considered electrically insulating. The walls of our enclosure consist of two spherical portions and two others offset from the vertical. To translate the parietal conditions more simply, it is therefore necessary to look for a curvilinear coordinate system in which the boundaries of our domain are parametrized by lines of constant coordinates. Thus, given the geometry of the containment, the most suitable coordinate system is that of bispherical coordinates. For a two-dimensional flow, the transition from Cartesian coordinates (x, y) to bispherical coordinates is given by the relation (1):

$$\begin{cases} x = \dfrac{a \sin\theta}{ch\eta - cos\theta} \\ y = \dfrac{a\, sh\eta}{ch\eta - cos\theta} \end{cases} \quad \ldots\ldots\ldots\ldots\ldots\ldots\ldots\ldots\ldots (1)$$

Along the vertical are two walls identified by θ = 0 and θ = π. The two internal and external hemispheres are respectively materialized by the coordinate lines h=hi and h=he.

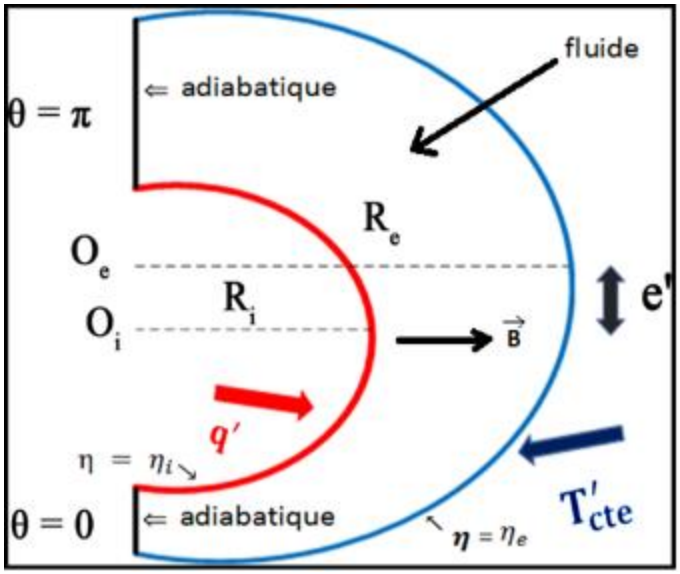

Figure 1 Geometry of the problem [19]

2.2. Governing equations

After introduction of the simplifying hypotheses, one establishes the various adimensional equations necessary to the resolution of the problem considered in this study. The vortex-flux (vortex flow) functions are translated by the momentum and heat equations translated by the relation (2):

$$\frac{\partial}{\partial t}\left(\frac{\Omega}{K}\right)+\frac{1}{H}\left[U-\frac{3PrG_2}{K}\right]\partial_\eta\left(\frac{\Omega}{K}\right)+\frac{1}{H}\left[V+\frac{3PrG_1}{K}\right]\partial_\theta\left(\frac{\Omega}{K}\right)=\frac{Pr}{H^2}\left[\partial_\eta^2\left(\frac{\Omega}{K}\right)+\partial_\theta^2\left(\frac{\Omega}{K}\right)\right]+\frac{RaPr}{KH}\left[G_2\,\partial_\eta T-G_1\,\partial_\theta T\right]+\frac{Ha^2Pr}{KH^2}\left[\partial_\eta\{H(UB_\eta B_\theta-VB_\eta^2)\}-\partial_\theta\{H(VB_\eta B_\theta-UB_\theta^2)\}\right] \quad \ldots\ldots\ldots\ldots\ldots\ldots\ldots\ldots (2)$$

Where the grandeur: U, V , G_1, G_2, K, H, B_η et B_θ are defined through the equations (3),(4), (5) et (6)

$$\begin{cases} U=\frac{1}{KH}\frac{\partial\Psi}{\partial\theta} \\ V=-\frac{1}{KH}\frac{\partial\Psi}{\partial\eta} \end{cases} \quad \ldots\ldots\ldots\ldots\ldots\ldots\ldots\ldots .(3)$$

$$\begin{cases} G_1=\frac{1-\cos\theta\,ch\eta}{ch\eta-\cos\theta} \\ G_2=-\frac{\sin\theta\,sh\eta}{ch\eta-\cos\theta} \end{cases} \quad \ldots\ldots\ldots\ldots\ldots\ldots\ldots\ldots (4)$$

$$\begin{cases} K=\frac{a\sin\theta}{D(ch\eta-\cos\theta)} \\ H=\frac{a}{D(ch\eta-\cos\theta)} \end{cases} \quad \ldots\ldots\ldots\ldots\ldots\ldots\ldots\ldots (5)$$

$$\begin{cases} B_\eta=G_2 \\ B_\theta=-G_1 \end{cases} \quad \ldots\ldots\ldots\ldots\ldots\ldots\ldots\ldots (6)$$

The condition of incompressibility is verified by flow functions: one surface noted Ψ and the other voluminal noted Φ. These flows are related by the equation (7):

$$\Psi = K\Phi \quad \ldots\ldots\ldots\ldots (7)$$

Otherwise, the equation of the flux function is known by the relation (8):

$$\Omega = \frac{1}{K^2 H}\left[G_2 \partial_\eta \Phi - G_1 \partial_\theta\right] - \frac{1}{KH^2}\left[\partial_\eta^2 \Phi - \partial_\theta^2 \Phi\right] \text{ ..... (8)}$$

To these different equations are added the boundary and initial conditions.

At t = 0, the conditions result in the relation (9):

$$\Omega = \Psi = T = U = V = 0 \text{ . ..... (9)}$$

At t > 0, the boundary conditions result in equations (10), (11) and (12) depending on the location of the wall.

- On the inner spherical wall (η = ηi)

$$\begin{cases} \Psi = U = V = 0 \\ \Omega = -\frac{1}{KH}\partial_\eta^2 \Psi \\ \partial_\eta T = H_i = \frac{ch\eta_i}{sh^2\eta_i} \end{cases} \text{ ..... (10)}$$

- On the outer spherical wall (η=ηe)

$$\begin{cases} \Psi = U = V = 0 \\ \Omega = -\frac{1}{KH}\partial_\eta^2 \Psi \end{cases} \text{ ..... (11)}$$

- On the two vertical walls (θ = 0, θ = π)

$$\begin{cases} \Psi = U = V = 0 \\ \partial_\eta T = 0 \\ \Omega = -\frac{1}{KH}\partial_\theta^2 \Psi \end{cases} \text{ ..... (12)}$$

The Nusselt number translates the thermal energy transmitted by a spherical wall. The local (Nu) and average ($\overline{(Nu)}$) Nusselt numbers are defined by the relations (13) and (14) according to the wall.

- For the inner spherical wall

$$\begin{cases} Nu_i = \frac{1}{T_{i,m}} \\ \overline{Nu_i} = \frac{1}{S_i}\int Nu_i dS_i \end{cases} \text{ ..... (13)}$$

- For an outer spherical wall

$$\begin{cases} Nu_e = \frac{1}{H_e T_{i,m}}\partial_\eta T \\ \overline{Nu_e} = \frac{1}{S_e}\int Nu_e d\, S_e \end{cases} \text{ ..... (14)}$$

2.3. Numerical analysis

For the development of a numerical code stimulating the magneto-convection of a Newtonian fluid confined in an annular space, we used:

- The implicit alternating directions (ADI) method for the temporal solution of the momentum and heat equations ;
- The finite difference method for spatial integration.

We will use the THOMAS algorithm for solving the system of linear equations obtained using ADI. However, for the equation of the flow function, the resolution is made based on the method of successive over-relaxation (SOR) with an optimal relaxation parameter. At the level of the iterative loop, the calculation result Z_{new} of a quantity to be determined will be considered as being a convergent solution only if it obeys, with the old value Z_{old} , the following relation (15):

$$\frac{|Z_{new}-Z_{old}|_{max}}{|Z_{new}|} \leq 10^{-5} \quad \text{..... (15)}$$

The steady state is reached only if this relative error between two consecutive time steps for all quantities obeys the relation (16):

$$\frac{|Z^{n+1}-Z^{n}|_{max}}{|Z^{n+1}|_{max}} \leq 10^{-5} \quad \text{..... (16)}$$

Where; Z^n represented Ω, Ψ or T to nth time step

3. Results and discussion

3.1. Computation Conditions

The choice of the 51 x 51 mesh and the 10-4 time step is motivated by tests carried out on the influence of the latter. The results of these tests are presented in Tables 1 and 2 and prove that these choices constitute, among other things, a good compromise.

Table 1 Effects of time steps on the Nusselt number of the heat wall for Ha=1, Ra = 105, e=0, Δt = 10-4 and the grid system is 51x51

	Time steps		
	10-3	**10-4**	**10-5**
Nu	4.7337	4.7298	4.7296
Difference (%)	0.087	0.004	0
Time computing (min)	5	124	802

Table 2 Effects of mesh refinement on the Nusselt number of the heat wall for Hart=1, Ra=105, e = 0 and Δt = 10-4

	Mesh grid							
	21*21	**21*41**	**41*41**	**41*51**	**41*81**	**51*51**	**51*81**	**81*81**
Nu	4.8750	4.8871	4.7515	4.7503	4.7502	4.7298	4.7297	4.7060
Difference (%)	3.59	3.85	0.97	0.94	0.94	0.51	0.50	0
Time computing (min)	9	97	225	261	362	348	447	604

3.2. Validation

For a zero magnetic field, the problem becomes that of laminar natural convection. The results presented in Table 3 provide information on the values of the mean Nusselt number, calculated and then given for different Rayleigh numbers. We compared these results with those of [19] for the study of transient laminar convection between two

vertically eccentric hemispheres. These comparisons show a relative difference of 02.72% for all the cases presented. This shows an excellent agreement between the results.

Table 3 Comparaison of the mean Nusselt number in a case of e = 0

	Ra				
	103	**104**	**105**	**106**	**107**
Nusselt number (our results)	2.0673	3.0379	4.8920	7.7680	11.708
Nusselt number (results of [19])	2.125	3.0651	4.982	7.6874	11.671
Difference (%)	2.72	0.89	1.81	1.05	0.32

3.3. Effect of eccentricity

At different values of eccentricity, temporal evolutions of isotherms and streamlines in the studied enclosure are presented side by side through Figures 2(a)-(c). The eccentricity takes the values {-0.5; 0; 0.5} and the Hartmann, Rayleigh and Prandtl numbers take the values 10, 106 and 0.7 respectively. They are fixed for the three eccentricity values studied. Initially, we observe an appearance of isotherms at the level of the heated internal wall. For the various values of the eccentricity, the isothermal lines deform over time. The heating of the fluid is done on the upper part of the internal wall before descending towards the external wall. The isothermal lines deform while increasing for a high value of the modified Rayleigh number. This increase is due to the movement of the fluid. However, the increase in the maximum value of the current function occurs with the eccentricity and becomes larger and larger for negative values. And the more the eccentricity increases by taking only negative values, the more the center of the vortex of the fluid focuses upwards. For an increase of the eccentricity towards positive values, the center of the vortex of the fluid will be observed downwards.

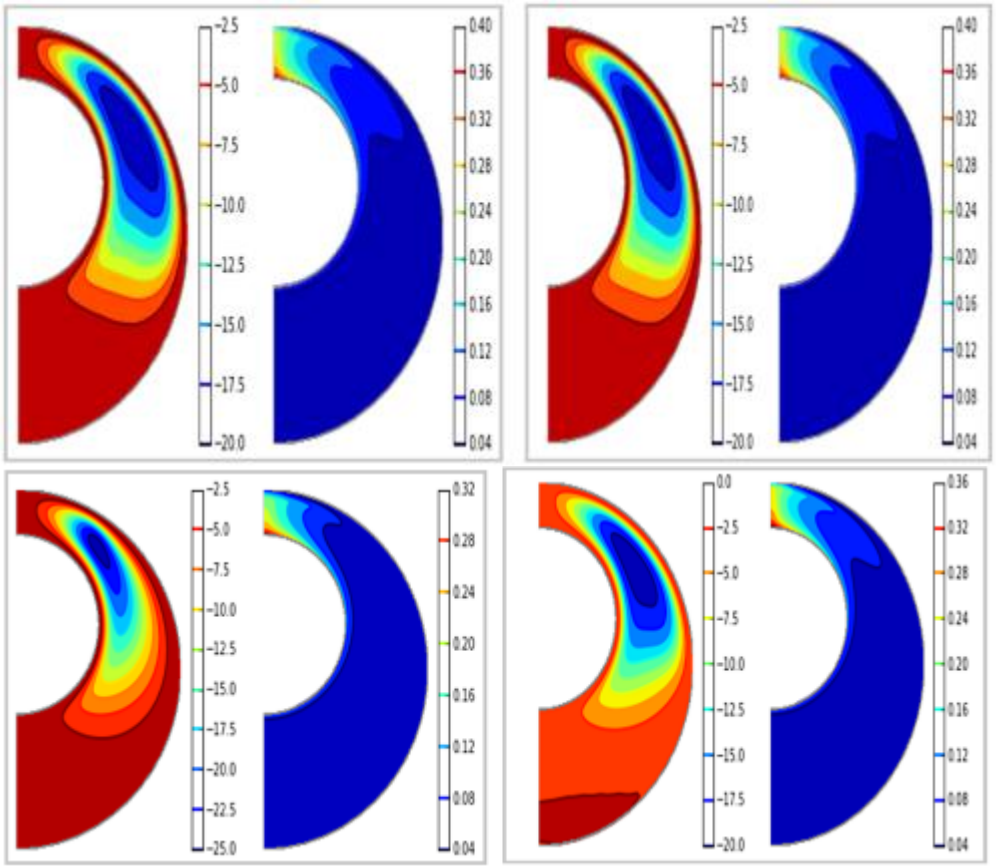

Figure 2 (a) Evolution of streamlines and isotherms for Ra=106, Hart=10, Pr=0.7 and e= − 0.5

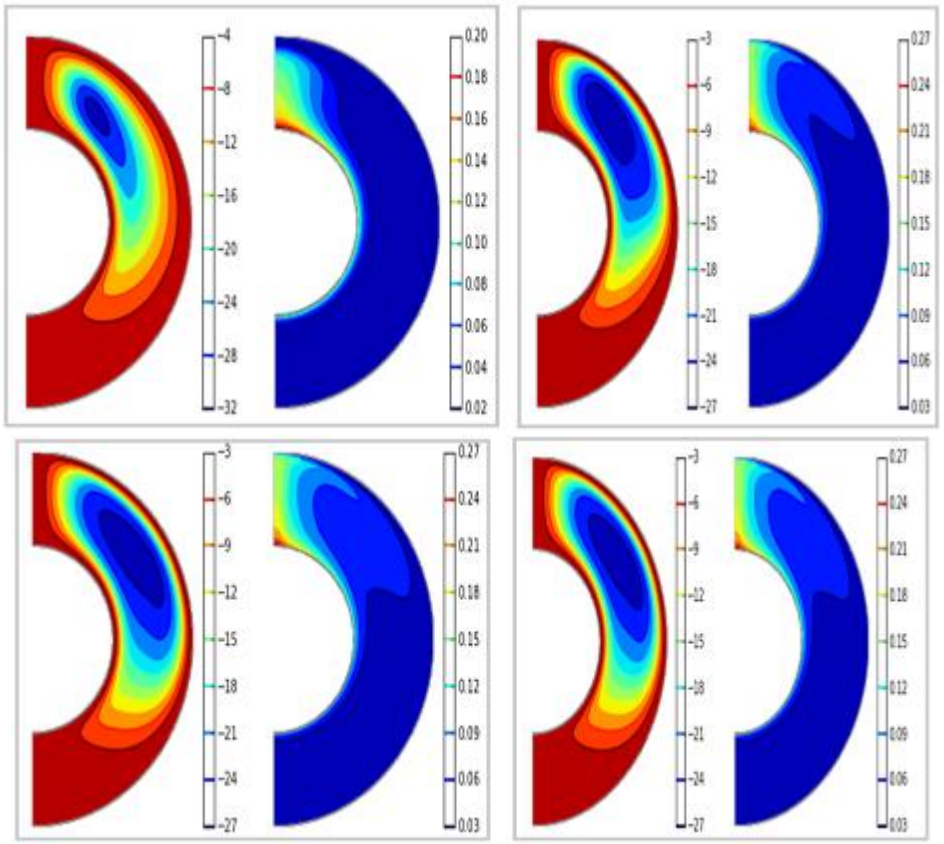

Figure 2 (b) Evolution of streamlines and isotherms for Ra=106, Hart =10, Pr=0.7 and e = 0

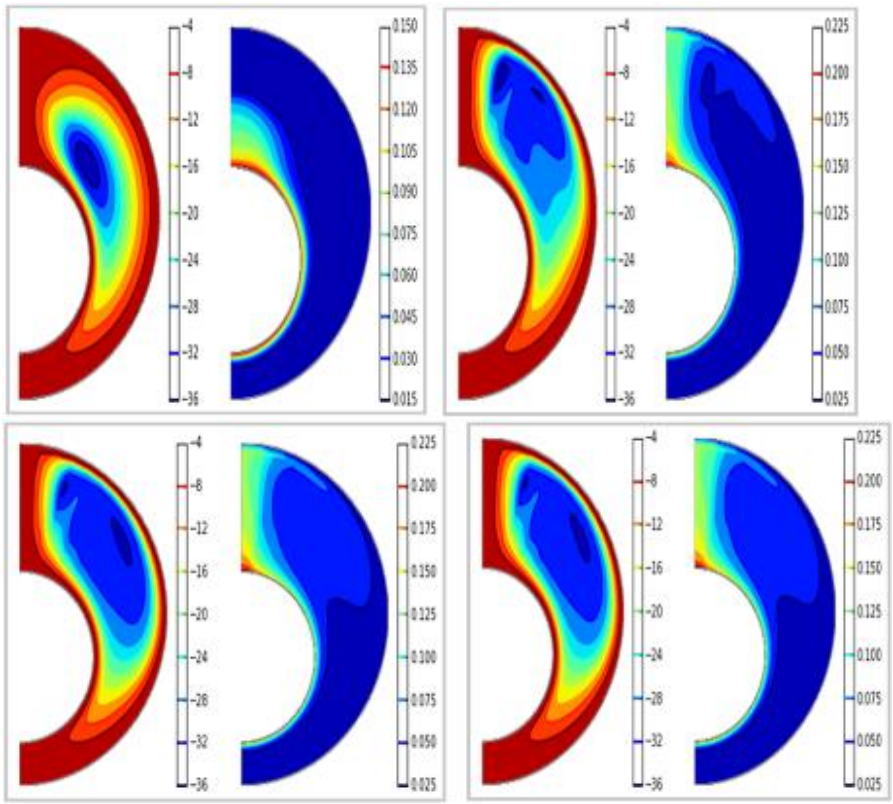

Figure 2 (c) Evolution of streamlines and isotherms for Ra=106, Hart =10, Pr=0.7 and e = 0.5

3.4. Hartmann number effect

Les figures 3(a)-(c) présentent l'évolution des isothermes et lignes de courant en fonction du temps pour les valeurs d'excentricité, Rayleigh et de Prandtl fixées, et différentes valeurs de Hartmann {1; 10; 100}. Il ressort de l'analyse que l'augmentation du nombre de Hartmann fortifie les lignes de courant et renforce le transfert le transfert de chaleur au niveau de l'enceinte. Le champ magnétique fait que la magnéto convection s'accompagne non seulement d'une importante énergie cinétique mais aussi d'un plus élevé taux de transfert de chaleur comparée à l'étude de la convection naturelle pure.

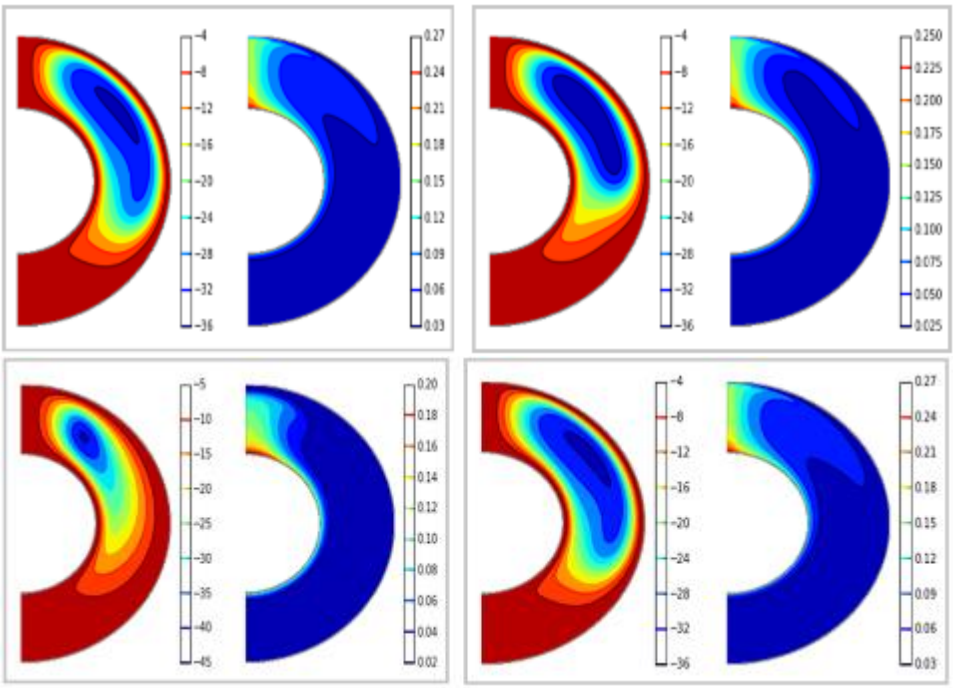

Figure 3 (a) Evolution of streamlines and isotherms for Ra=106, Pr=0.7, e= 0.5 and Hart=1

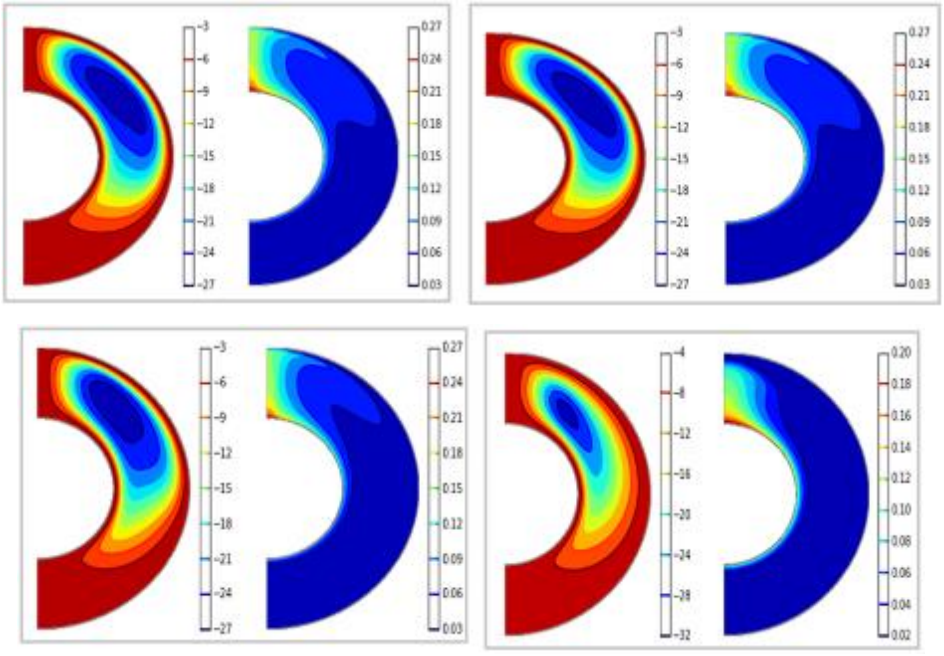

Figure 3 (b) Evolution of streamlines and isotherms for Ra=106, Pr=0.7, e= 0.5 and Hart=10

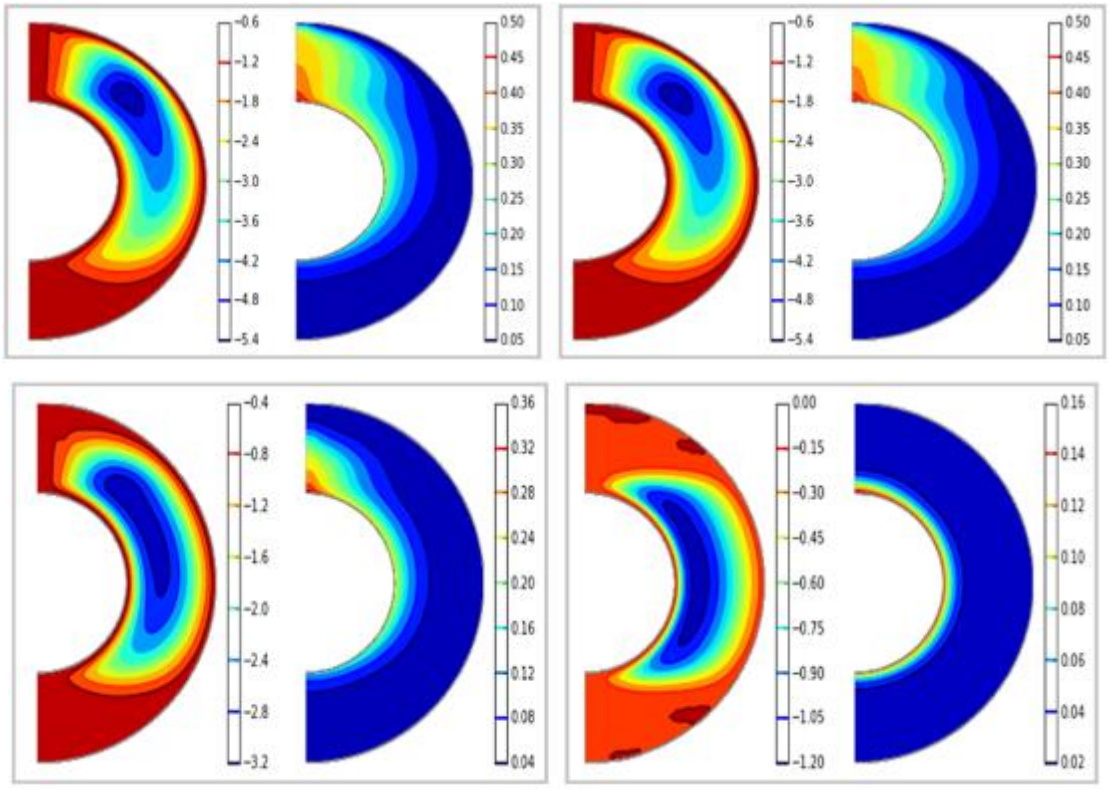

Figure 3 (c) Evolution of streamlines and isotherms for Ra=106, Pr=0.7, e= 0.5 and Hart=100

3.5. Influence of Rayleigh number

For a fixed Hartmann number in each case, the zero eccentricity and Rayleigh numbers varying from 103 to 106, the curves in Figures 3 (a) - (c) above give the variation of the mean Nusselt number respectively, of the minimum current function and the average temperature of the inner wall as a function of time. Through figure 3(a) we observe the evolution of the average Nusselt number on the inner hemisphere as a function of dimensionless time. This variation proves that the average Nusselt number decreases before becoming monotonic. For a Rayleigh number equal to 106, the mean Nusselt number is lower than that obtained in the case of the non-conductive fluid [16]. Figure 3(c) gives the evolution of the dimensionless average temperature of the inner wall for Rayleigh numbers equal to $\{10^3; 10^4; 10^5; 10^6\}$. It shows that for a given Rayleigh number, this dimensionless average temperature increases with dimensionless time before becoming monotonous after a few moments. However, we will also note its decrease for larger Rayleigh numbers. Moreover, our values are slightly higher than those of [9] and [19]. For the same Rayleigh numbers that we used previously, Figure 3(b) gives, as a function of dimensionless time, the evolution of the minimum flux function. The latter decreases rapidly before stabilizing when the steady state is reached. This decrease is much greater for higher values of the Rayleigh number. If the latter takes the values 105 and 106, the curves present peaks before stabilizing. The explanation that we can make to this phenomenon is that at the beginning thanks to the initial conditions and the limits of the system, the convection becomes predominant and this creates an important movement of the fluid. As soon as the stationary regime is reached, these magneto-convective phenomena are attenuated.

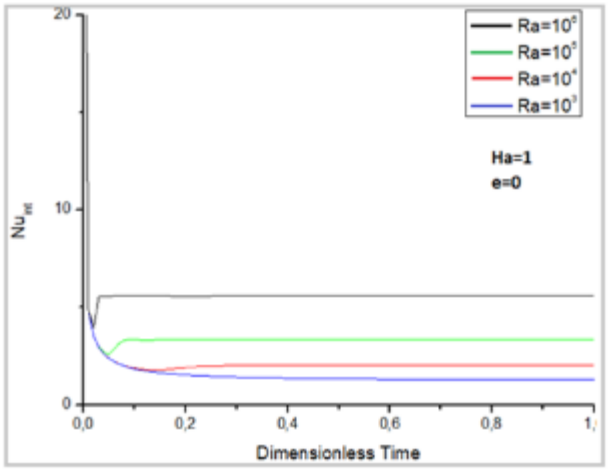

Figures 3 (a) Temporal variation of the average Nusselt nomber for various values of Ra

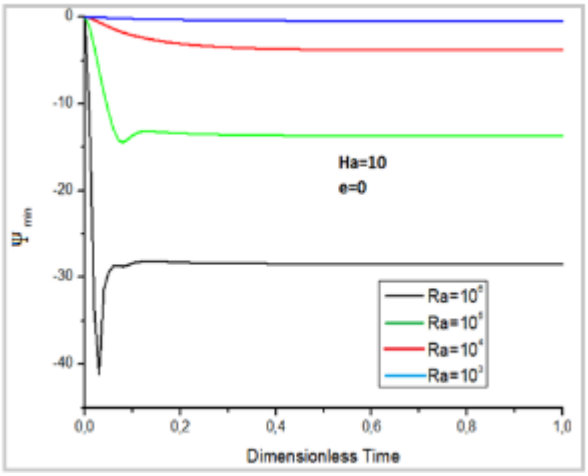

Figure 3 (b) Temporal variation of the minimum current function for various values of Ra

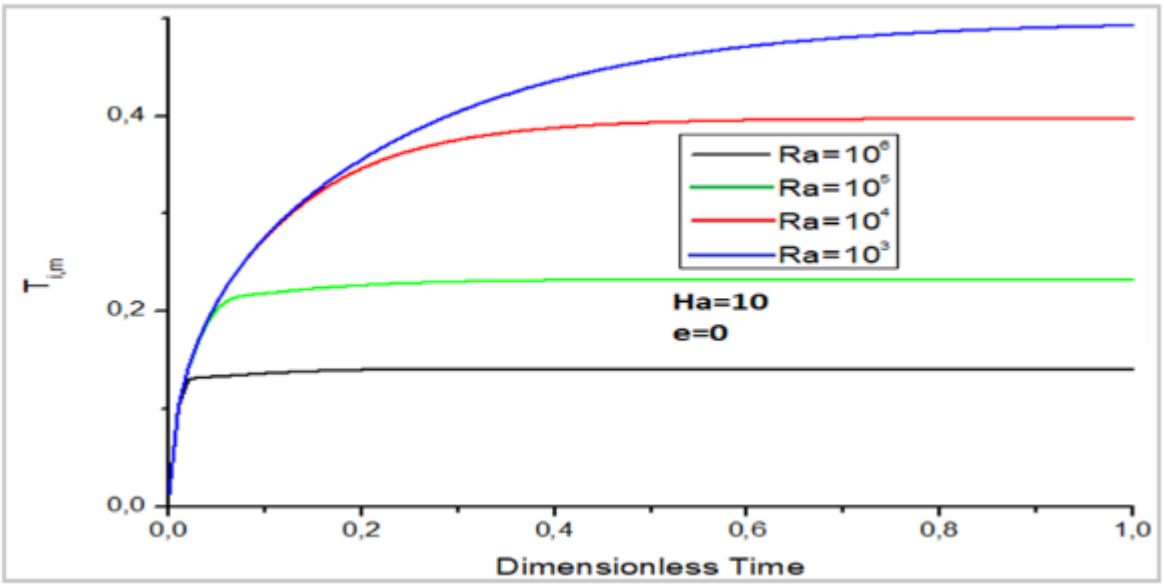

Figure 3 (c) Temporal variation of mean inner wall temperature for various values of Ra

3.6. Influence of Eccentricity

Figure 4-(a) gives the evolution of the mean Nusselt number on the inner wall, Figure 4-(b) displays the variation of the minimum flux function and Figure 4-(c) presents the evolution of dimensionless temperature. All these curves depend on dimensionless time for various values of the eccentricity, a Rayleigh number equal to 106 and a Hartmann number equal to unity. In steady state, the average Nusselt number on the inner hemisphere decreases with negative values of the eccentricity e. However, this number becomes higher for positive eccentricities. As for the minimal flux function, for a given eccentricity, it decreases rapidly as a function of dimensionless time and then increases before becoming monotonous when the stationary state is reached. For various values of the eccentricity, the minimum of the flux function decreases for higher values of the eccentricity. The average temperature at the heated wall as a function of dimensionless time actually depends on the configuration, i.e. on the eccentricity. So for a given eccentricity, this temperature increases rapidly then slowly before stabilizing when the stationary state is reached. For negative values of the eccentricities, the temperature decreases with this one. On the other hand, we observe an increase in the average temperature on the heated inner hemisphere with positive values of the eccentricity.

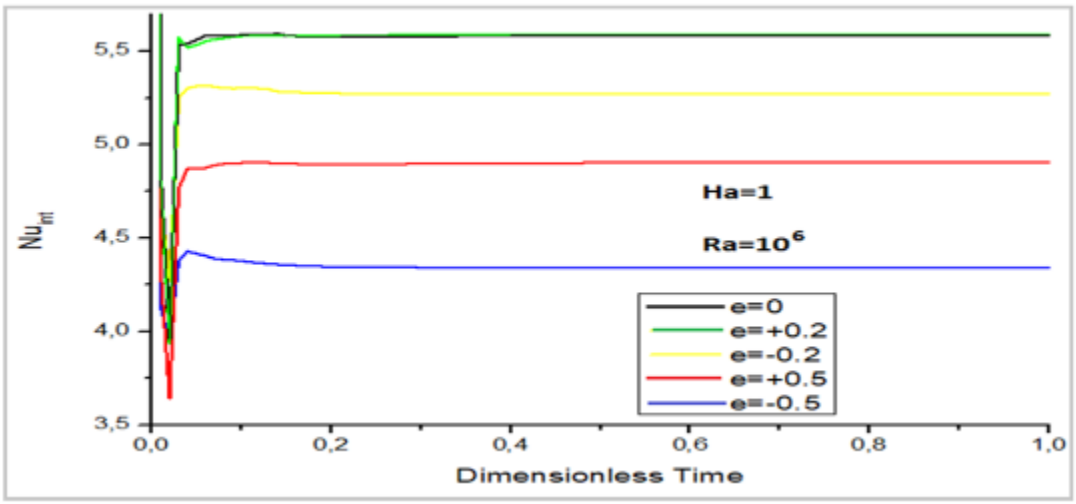

Figure 4 (a) Influence of eccentricity on the mean Nusselt number of the heated wall as a function of dimensionless time

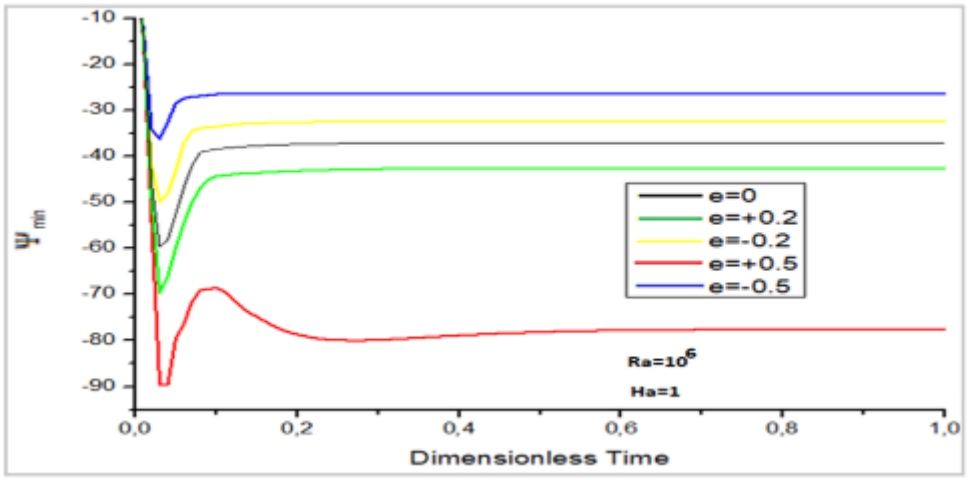

Figure 4 (b) Influence of eccentricity on minimum running current as a function of dimensionless time

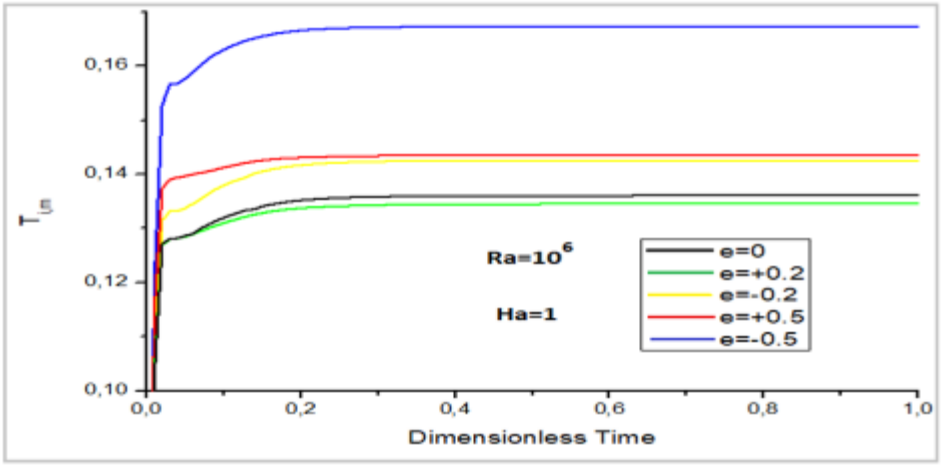

Figure 4 (c) Influence of eccentricity on the dimensionless mean temperature as a function of dimensionless time

3.7. Influence of Hartmann number

Figures 5(a)-(c) display respectively for a fixed Rayleigh number and eccentricity and various values of the Hartmann number, the evolution of the mean Nusselt number on the inner hemisphere, the variation of its minimum function of flux and that of the mean temperature as a function of dimensionless time. Curve 5-(a) allows us to state that for each Hartmann number, the average Nusselt number on the heated wall decreases rapidly then increases before stabilizing. The shapes of these Nusselt number evolution curves are identical to those observed in the case of pure natural convection as shown by the results of [19]. However, it is important to note that in the case of magneto convection, the presence of the magnetic field gives lower values of the average Nusselt number on the inner hemisphere. And the larger this field, i.e. for large values of the Hartmann number, the Nusselt number becomes increasingly weak. Figure 5-(b) also shows that for a constant value of the Hartmann number, the minimum flux function decreases then increases before being constant. The decrease of this minimal flux function is small for small Hartmann numbers. The minimum flux function decreases if the Hartmann number increases. Figure 5-(c) gives the evolution of the dimensionless mean temperature of the inner hemisphere as a function of time, also dimensionless, for various values of the Hartmann number. For low times, the value of the Hartmann number has no influence on that of the dimensionless average temperature. For a long time, this temperature of the inner hemisphere increases with the Hartmann number. The existence of the magnetic field further warms the inner hemisphere.

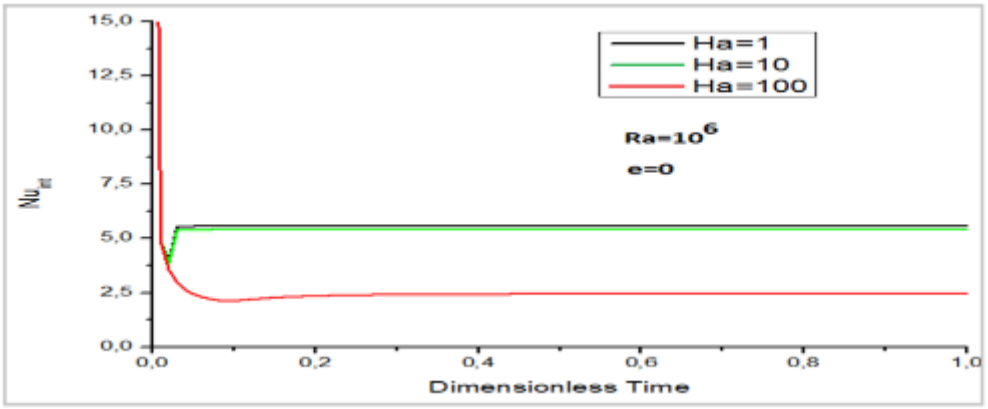

Figure 5 (a) Evolution of the average Nusselt number on the inner hemisphere as a function of dimensionless time

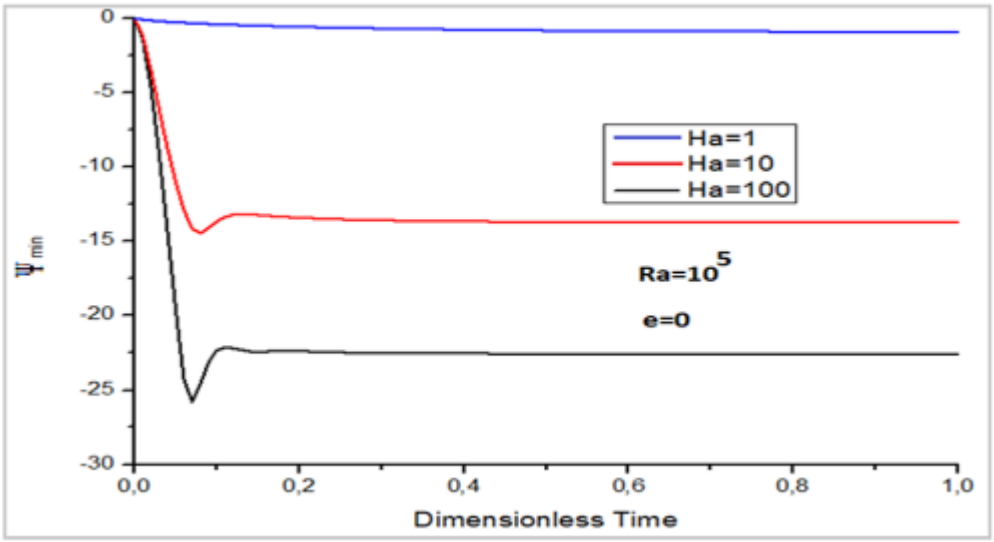

Figure 5 (b) Evolution of its minimal flux function as a function of dimensionless time

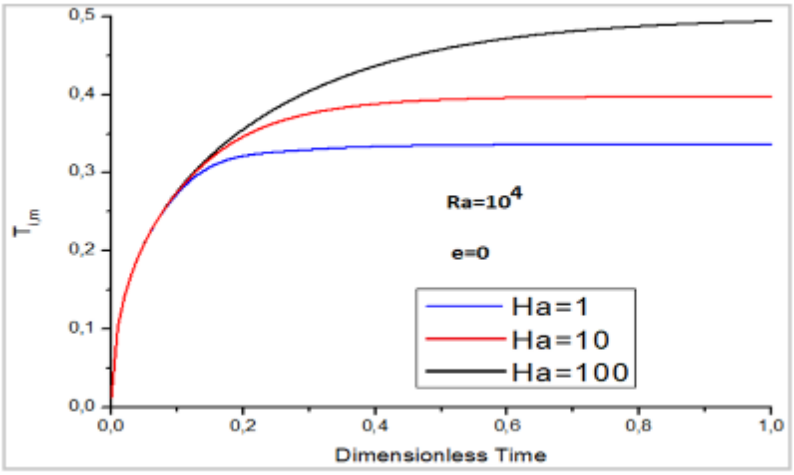

Figure 5 (c) Evolution of the mean temperature as a function of dimensionless time

Nomenclature

- a, parameter of torus pole (m)
- e, eccentricity
- g, gravity intensity ($m \cdot s^{-2}$)
- g_1 and g_2 coefficients
- H and K, metrics coefficient dimensionless
- B_0, Magnetic field strength ($N/A\ m^2$)
- Ha, Hartmann number
- Nu_e, Nusselt number for the outer hemisphere
- Nu_i, Nusselt number for the inner hemisphere
- O_i and O_e respectively center of inner and outer hemisphere
- Pr, Prandtl number
- q, Heat flux density ($W.m^{-2}$)
- Ri and Re, respectively radius of inner and outer hemisphere
- Ra, Rayleigh number
- t, dimensionless time
- t', dimension time, (s)
- T, dimensionless temperature
- U and V, dimensionless velocity components in the transformed planes
- x and y, cartesian coordinates, (m)
- α, thermal diffusivity, ($m^2.s^{-1}$)
- β, thermal expansion coefficient, (K^{-1})
- σ, electrical conductivity, ($A.m.V^{-1}$)
- Δt, time step, (s)
- ΔT, difference of temperatures between the two hemispheres, (K)
- η and θ, bispherical coordinates, (m)
- λ, thermal conductivity, ($W.K^{-1}.m^{-1}$)
- ν, kinematical viscosity, ($m^2.s-1$)
- Ψ, dimensionless stream-function,
- Ψ', dimension stream-function, ($m^3.s^{-1}$)
- Ω, dimensionless vorticity,
- Ω', dimension vorticity, ($m^3.s^{-2}$)

4. Conclusion

In this article, we have numerically studied the magneto-convection of a fluid, confined between two eccentric hemispheres. The studied hemispherical cavity is subjected to thermal and electrical boundary conditions in order to obtain the critical values of the parameters marking the beginning of the instability. This is to highlight the effect of the external magnetic field on the speed and heat transfer. For this purpose, a constant heat flux density is imposed on the

inner hemispherical wall and a constant temperature on the outer hemisphere. The equations which govern the magneto-convection, are projected in the bispheric coordinates. Discretization by the finite difference method facilitated the development of a computer code in Fortran. Solving the equations is done using the ADI and SOR methods. Assumptions are made on the vorticity and flux function variables. For very weak magnetic fields, magneto convection comes down to a problem of natural convection. At the end of the study, the results obtained are consistent and revealing: Just as in the case of pure natural convection, the geometry of the system studied reveals that different values of eccentricity give effects on the magneto-convection of a fluid subjected to a constant horizontal magnetic field. The center of the vortex points towards the top of the enclosure for negative values of the eccentricity and towards the bottom for positive values. Increasing the modified Rayleigh number enlarges the value of the Nusselt number but it decreases the dimensionless temperature on the inner hemisphere for a given configuration. As for the flux function, it becomes increasingly weak for one of the larger eccentricities. For a given configuration, not only does the increase in the Hartmann number orient the center of the vortex, in its movement from the inner hemispherical wall to the outer one, a little more towards the central part, but it also slightly decreases the value of the number of Nusselt on the wall of the heated internal hemisphere while facilitating the progression of this heat inside the domain considered. Moreover, our results are in good conformity with the solutions available in the literature such as [9], [19], etc.

Compliance with ethical standards

Acknowledgments

I would like to sincerely thank Professor Mamadou Lamine SOW who did me the honor of supervising this doctoral thesis from which this article is taken. I would also like to thank all my co-authors who spared no effort to bring this document to fruition. Finally, I would like to thank Mr. Pape Sene who took full responsibility for the publication.

Disclosure of conflict of interest

The authors declare no conflicts of interest regarding the publication of this paper.

References

[1] Shelyag S, Schüssler M, Solanki SK , Berdyugina SV, Vögler A. G-band spectral synthesis and diagnostics of simulated solar magneto-convection. 2004; 427 : 335–343

[2] Jamai H , Fakhreddine S O, Sammouda H. Numerical Study of Sinusoidal Temperature in Magneto-Convection. Journal of Applied Fluid Mechanics. 2014; 7(3): 493-502.

[3] Sathiyamoorthy M, Ali C. Effect of magnetic field on natural convection flow in a liquid gallium filled square cavity for linearly heated side walls. International Journal of Thermal Sciences. 2010; 49: 1856-1865.

[4] Zanella R , Nore C, Bouillault F, Mininger X, Guermond J L , Tomas I, Cappanera L. Numerical study of the impact of magnetoconvection on the cooling of a coil by ferrouid", Non Linéaire Publications, Avenue de l'Université, BP 12, 76801 Saint-Etienne du Rouvray cedex; 2017.

[5] Umadevi P, Nithyadevi N. Magneto-convection of water-based nanofluids inside an enclosure having uniform heat generation and various thermal boundaries. Journal of the Nigerian Mathematical Society. 2016; 35: 82–92.

[6] Gelfgat A, Zikanov Y O. Computational modeling of magneto-convection: Effects of discretization method, grid refinement and grid stretching. Computers and Fluids. 2018; 1–17.

[7] Sarr J, Mbow C, Chehouani H, Zeghmati B, Benet S, Daguenet M. Study of Natural Convection in an Enclosure Bounded by Two Concentric Cylinders and Two Diametric Planes. Journal of Heat Transfer. 1995; 117: 130-137.

[8] Shin T. Penetration of Alfvén waves into an upper stably-stratified layer excited by magnetoconvection in rotating spherical shells . Physics of the Earth and Planetary Interiors. 2015; 241: 37–43.

[9] Mamadou LS , Joseph S, Cheikh M, Babacar M, Bernard C, Mamadou M K. Geometrical and Rayleigh Number Effects in the Transient Laminar Free Convection between Two Vertically Eccentric Spheres. International Journal of Numerical Methods for Heat & Fluid Flow. 2009; 19: 689-704.

[10] Mack L R, Hardee H.C. Natural Convection between Concentric Spheres at Low Rayleigh Numbers. International Journal of Heat and Mass Transfer. 1968; 11: 387-396.

[11] Tazi MN, Daoudi S, Palec GL, Daguenet M. Numerical study of the Boussinesq model of permanent axisymmetric laminar natural convection in an annular space between two spheres. General Review of Thermal. 1997 ; 36: 239-251.

[12] Rainer Hollerbach A. A spectral solution of the magneto-convection equations in spherical geometry", International Journal for Numerical Methods in Fluids. 2000; 32: 773-797.

[13] Shelyag S , Schüssler M , Solanki S K, Vögler A. Stokes diagnostics of simulated solar magneto-convection. . 2007; 469: 731–747.

[14] Dulal P, Sewli C. Mixed convection magnetohydrodynamic Heat and mass transfer past a stretching surface in a micropolar fluid-saturated porous medium under the influence of ohmic heating, Soret and Dufour effects. Commun Nonlinear Sci Numer Simulat. 2011; 16:1329–1346.

[15] Das S, Guchhait S K , Jana RN, Makinde OD. Hall effects on an unsteady magneto-convection and radiative heat transfer past a porous plate. Alexandria Engineering Journal. 2016; 55: 1321–1331.

[16] Ozoe H , Okada K. The effect of the direction of the external magnetic field on the three-dimensional natural convection flow in a cubical enclosure. International Journal of Heat and Mass Transfer. 1989; 32: 1939-1954.

[17] Venkatachalappa M, Subbaraya CK. Natural convection in a rectangular enclosure in the presence of magnetic field with uniform heat flux from side walls. Acta Mechanica. 1993; 96: 13-26.

[18] Dulal P. Mixed convection heat transfer in the boundary layers on an exponentially stretching surface with magnetic field. Applied Mathematics and Computation. 2010; 217 (6): 2356-2369

[19] Koita MN, Sow ML, Thiam ON, Traoré VB, Mbow C , Sarr J. Unsteady Natural Convection between Two Eccentric Hemispheres. Open Journal of Applied Sciences. 2021; 11: 177-189.

[20] Vögler A, Shelyag S, Schüssler M, Cattaneo F, Emonet T, Linde T. Simulations of magneto-convection in the solar photosphere. Equations, methods, and results of the MURaM code. 2004; 429: 335–351.